

# Contributions of Muscle Imbalance and Impaired Growth to Postural and Osseous Shoulder Deformity Following Brachial Plexus Birth Palsy: A Computational Simulation Analysis

Wei Cheng, MS, Roger Cornwall, MD, Dustin L. Crouch, PhD, Zhongyu Li, MD, PhD, Katherine R. Saul, PhD

**Purpose** Two potential mechanisms leading to postural and osseous shoulder deformity after brachial plexus birth palsy are muscle imbalance between functioning internal rotators and paralyzed external rotators and impaired longitudinal growth of paralyzed muscles. Our goal was to evaluate the combined and isolated effects of these 2 mechanisms on transverse plane shoulder forces using a computational model of C5–6 brachial plexus injury.

**Methods** We modeled a C5–6 injury using a computational musculoskeletal upper limb model. Muscles expected to be denervated by C5–6 injury were classified as affected, with the remaining shoulder muscles classified as unaffected. To model muscle imbalance, affected muscles were given no resting tone whereas unaffected muscles were given resting tone at 30% of maximal activation. To model impaired growth, affected muscles were reduced in length by 30% compared with normal whereas unaffected muscles remained normal in length. Four scenarios were simulated: normal, muscle imbalance only, impaired growth only, and both muscle imbalance and impaired growth. Passive shoulder rotation range of motion and glenohumeral joint reaction forces were evaluated to assess postural and osseous deformity.

**Results** All impaired scenarios exhibited restricted range of motion and increased and posteriorly directed compressive glenohumeral joint forces. Individually, impaired muscle growth caused worse restriction in range of motion and higher and more posteriorly directed glenohumeral forces than did muscle imbalance. Combined muscle imbalance and impaired growth caused the most restricted joint range of motion and the highest joint reaction force of all scenarios.

**Conclusions** Both muscle imbalance and impaired longitudinal growth contributed to range of motion and force changes consistent with clinically observed deformity, although the most substantial effects resulted from impaired muscle growth.

**Clinical relevance** Simulations suggest that treatment strategies emphasizing treatment of impaired longitudinal growth are warranted for reducing deformity after brachial plexus birth palsy. (*J Hand Surg Am.* 2015;40(6):1170–1176. Copyright © 2015 by the American Society for Surgery of the Hand. All rights reserved.)

**Key words** Brachial plexus birth palsy, shoulder deformity, computer simulation, muscle strength, impaired growth.

From the Department of Mechanical and Aerospace Engineering and the Department of Biomedical Engineering, North Carolina State University, Raleigh; and the Department of Orthopaedic Surgery, Wake Forest School of Medicine, Winston-Salem, NC; and the Division of Orthopedic Surgery, Cincinnati Children's Hospital Medical Center, Cincinnati, OH.

Received for publication November 17, 2014; accepted in revised form February 5, 2015.

No benefits in any form have been received or will be received related directly or indirectly to the subject of this article.

**Corresponding author:** Katherine R. Saul, PhD, Department of Mechanical and Aerospace Engineering, North Carolina State University, 911 Oval Drive, Engineering Building 3, Campus Box 7910, Raleigh, NC 27695-7910; e-mail: [ksaul@ncsu.edu](mailto:ksaul@ncsu.edu).

0363-5023/15/4006-0016\$36.00/0

<http://dx.doi.org/10.1016/j.jhssa.2015.02.025>

**B**RACHIAL PLEXUS BIRTH PALSY IS A perinatal injury to the peripheral nerves supplying the muscle of the upper limb, estimated to affect 0.4 to 4 per 1,000 newborns.<sup>1</sup> Injury most commonly occurs at the C5–6 level, resulting in paralysis of elbow flexors and muscles crossing the shoulder.<sup>2</sup> Postural and osseous deformities, including contractures of the shoulder and elbow,<sup>3,4</sup> abnormal morphology of the scapula and humerus, and subluxation of the humeral head,<sup>5–7</sup> are common sequelae of the nerve injury, even when spontaneous nerve regeneration is observed. Such deformity has a substantial negative impact on patient function and quality of life and motivates improved understanding of the etiology of the deformity to enhance treatment.

Recent literature suggests 2 potential muscular mechanisms underlying the clinically observed postural and osseous deformity: muscle imbalance and impaired longitudinal muscle growth. One long-held hypothesis suggests that the imbalance between paralyzed external rotators and intact internal rotator muscles at the shoulder leads to the internal rotation contractures, or restricted range of motion (ROM) and increased joint stiffness, that have been observed.<sup>1,2,8</sup> More recently, experiments in rodent models suggested that perinatal nerve injury may result in impaired longitudinal growth of the paralyzed muscles, resulting in reduced resting fiber length and overstretched sarcomeres.<sup>9,10</sup> A recent computational sensitivity analysis<sup>11</sup> investigating the potential biomechanical influence of these mechanisms on the joint reaction forces at the glenoid and on shoulder ROM suggested that both mechanisms have the potential to influence glenoid force, whereas impaired longitudinal growth may influence ROM. However, in that study, the roles of individual muscles were studied; it is unknown whether the combined effect of both mechanisms acting through multiple muscles has a potentially synergistic influence.

The goal of this study was to evaluate the combined and isolated effects of impaired longitudinal growth and muscle imbalance using a computational model of C5–6 brachial plexus injury on transverse plane mechanical forces at the shoulder. The model represented the clinically observed pattern of injury and muscle changes based on the best available descriptions of normal neuroanatomy, data from experimental animal models, and previously published clinical findings. In particular, we evaluated the effect of each mechanism on shoulder rotation ROM and transverse plane joint reaction forces at the glenohumeral joint.

## MATERIALS AND METHODS

We implemented simulations of brachial plexus birth palsy using a computational model of the upper limb,<sup>12,13</sup> as previously augmented for dynamic simulation of brachial plexus palsy.<sup>11</sup> Simulations were performed in OpenSim (version 3.1, Stanford, CA),<sup>14</sup> an open-source musculoskeletal simulation software platform. Briefly, the model integrates representations of bone and joint geometry for the shoulder, elbow, forearm, and wrist with models of the path and force-generating capacity of the 32 muscles crossing these joints. The muscles crossing the glenohumeral joint include the anterior deltoid, middle deltoid, posterior deltoid, teres major, teres minor, supraspinatus, infraspinatus, subscapularis, pectoralis major (clavicular head and 2 compartments of sternocostal head), biceps (long and short heads), triceps (long head), latissimus dorsi (3 compartments), and coracobrachialis. The subscapularis muscle was augmented from a previous implementation of the model to include 2 compartments: an upper compartment that accounts for one third of the total muscle mass, and a lower compartment accounting for two thirds of the muscle mass.<sup>15</sup> The origin-to-insertion paths of the muscles are based on anatomical description and experimental measurements of muscle moment arm,<sup>12</sup> which is the distance from the muscle line of action to the center of rotation of the joint. The force of each muscle actuator depends on posture of the arm, the level of muscle activation from unactivated (0%) to fully activated (100%), and architectural characteristics of the individual muscle. These characteristics include optimal muscle fiber length, peak isometric force (related to muscle physiologic cross-sectional area), pennation angle, and tendon length, and are derived from experimental measurements made from cadaveric specimens and MRIs of living subjects.<sup>16–22</sup> Representations of ligaments and other passive structures were included to limit movement at the extremes of the ROM.<sup>13,23</sup> The model permits calculation of joint moment, the product of muscle force and moment arm, which indicates a muscle's ability to contribute to or resist rotation at a joint.

We classified muscles crossing the shoulder as either affected or unaffected by a C5–6 level injury (Table 1), according to neuroanatomy, available clinical findings, magnetic resonance imaging (MRI), electrodiagnostic testing, muscle biopsies, and motion analysis.<sup>6–10,15,24–30</sup> “Affected” refers to initial denervation from the neurological injury, regardless of whether reinnervation occurs. “Unaffected” refers to muscles without interruption of innervation from

**TABLE 1. Affected and Unaffected Muscle Classifications**

Affected Muscles	Unaffected Muscles
Supraspinatus	Teres major*
Infraspinatus	Triceps (all heads)
Teres minor	Pectoralis major
Subscapularis (2 compartments)*	Latissimus dorsi
Deltoid	All other muscles
Long head of biceps	crossing elbow and
Short head of biceps	wrist
Brachialis	
Coracobrachialis	

\*Two versions of the simulations were considered: with subscapularis (2 compartments) and the teres major affected, and with the upper subscapularis affected while the middle/lower subscapularis and teres major are unaffected.

the neurological insult. We used the model to test 4 scenarios representing patterns of impaired longitudinal growth and muscle strength imbalance in isolation and combination (Table 2). Scenario 1 used the nominal model and represented an uninjured control. Scenario 2 represented isolated strength imbalance, in which muscles affected in a C–6 injury were permitted to produce passive force only, whereas unaffected muscles were activated to 30% of maximal possible activation; this value was based on the largest degree of imbalance described in a radiographic study of internal and external rotators.<sup>8,11</sup> Scenario 3 represented impaired growth of the muscles affected by a C–6 injury, in which impaired growth was represented by shortening the optimal fiber length by 30%; this value was selected based on reported muscle length deficits in affected muscles in a murine model of brachial plexus birth palsy.<sup>10,11</sup> Scenario 4 represented the combined influence of both impaired longitudinal growth and muscle strength imbalance following a C–6 injury if both mechanisms are in fact contributing to deformity. The influence of C5–6 injury on the subscapularis and teres major muscles is unclear. Therefore, we performed the simulations twice: first with both muscles treated as affected, and then with the upper muscle belly of the subscapularis affected and the middle and lower subscapularis muscle belly and teres major unaffected.

We evaluated the effect of each pattern of muscle changes on postural deformity by assessing the range of internal/external shoulder rotation permitted under each simulation scenario. We simulated the clinical examination of axial rotation ROM with the shoulder adducted and the elbow flexed to 90°. We calculated

the net joint moment generated by muscles and ligaments crossing the shoulder as the shoulder was moved across the ROM. The limit of the ROM was defined as the joint angle at which the muscles and ligaments crossing the shoulder exerted sufficient passive force to restrict shoulder rotation against a 3.5-kg load applied at the wrist; this method has been previously used experimentally to determine shoulder rotation range of motion.<sup>31</sup>

We evaluated the potential of each pattern of muscle changes to contribute to osseous deformity by assessing the compressive glenohumeral joint force. Forces that change to be more posteriorly directed are consistent with clinically observed posterior humeral head subluxation and glenoid retroversion. The joint force was calculated as the sum of gravitational and muscle forces transmitted between the humeral head and glenoid. For joint force calculations, the torso was oriented in an upright posture, the arm was placed in a neutral shoulder posture, and the elbow was permitted to flex freely. We calculated the joint forces exerted in the transverse plane and compared the magnitude and direction of these forces between simulation scenarios.

## RESULTS

In all injury scenarios, shoulder rotation ROM was restricted. Muscle imbalance alone resulted in the least restricted ROM, with external rotation reduced only 24° (scenario2 in Fig. 1). In contrast, combined strength imbalance and impaired growth (scenario4v1 in Fig. 1) resulted in more restricted ROM, especially for external rotation, which was reduced by 60°. When all compartments of subscapularis were considered to be affected (scenario3v1 and scenario4v1 in Fig. 1), ROM was restricted more than when only the upper compartment was affected. Specifically, ROM was restricted for the impaired growth only (scenario3 in Fig. 1) and combined (scenario4 in Fig. 1) mechanisms by 11° and 9° more, respectively, when subscapularis was considered totally affected.

Similarly, in all scenarios with altered muscle forces, the glenoid experienced substantially increased compressive and more posteriorly oriented joint reaction forces compared with the uninjured scenario. Whereas strength imbalance alone resulted in increased compressive forces (scenario2 in Fig. 2) that were more posterior than the uninjured scenario (84° posterior to unimpaired scenario1 in Fig. 2), impaired longitudinal growth resulted in much higher forces (scenario3v1 in Fig. 2; 123% higher than scenario2 in Fig. 2) that were oriented in a more posterior direction

**TABLE 2. Simulation Scenarios**

	Affected	Unaffected	Mechanisms
1	No change	No change	
2	Normal length, 0% activation	Normal length, 30% activation	Muscle imbalance
3	Short, 0% activation	Normal length, 0% activation	Impaired growth
4	Short, 0% activation	Normal length, 30% activation	Both

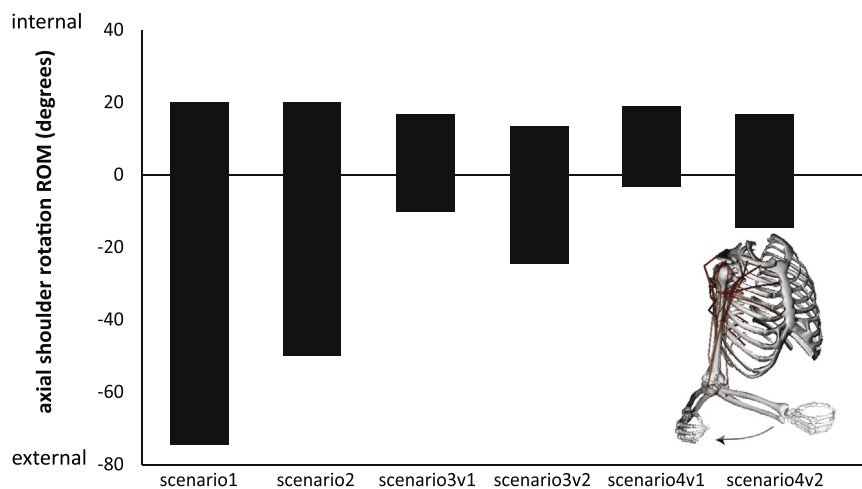


**FIGURE 1:** Passive ROM for axial shoulder rotation. Muscle imbalance (scenario2) restricted external rotation ROM relative to the unimpaired case (scenario1) but did not restrict internal rotation. Cases in which impaired growth was applied to affected muscles (scenario3) or in concert with muscle imbalance (scenario4) exhibited restrictions of both internal and external rotation ROM. Cases in which the subscapularis and teres major were completely affected (scenario3v1 and scenario4v1) had more substantial external rotation ROM restrictions compared with when only upper subscapularis was affected (scenario3v2 and scenario4v2).

(scenario3v1 in Fig. 2; 87° posterior to scenario1 in Fig. 2). The combined influence of muscle imbalance and impaired growth resulted in larger and more posteriorly directed forces than either mechanism alone; for example, scenario4v1 in Fig. 2 was directed at 101° posterior to the unimpaired case, with 257% higher forces than the muscle imbalance mechanism alone (case 2 in Fig. 2) and 61% higher forces than the impaired growth of affected muscles mechanism alone (case 3v1 in Fig. 2). When subscapularis was considered to be only partially affected and teres major unaffected (cases 3v2 and 4v2 in Fig. 2) forces were reduced in magnitude (7% and 2% reduced for cases 3 and 4, respectively, in Fig. 2) and less posteriorly directed (13° and 4°, respectively).

## DISCUSSION

Our simulations revealed that both muscle imbalance and impaired longitudinal growth change glenohumeral passive ROM and joint reaction forces, which is consistent with clinically observed patterns

of postural and osseous deformity. Whereas earlier work with this computational model<sup>11</sup> also investigated the influence of the 2 mechanisms under consideration here, it focused on the roles of individual muscles without investigating the relative impact of the 2 mechanisms in isolation or combination. The current study showed that the combined influence of both imbalance and impaired growth was larger than either in isolation, and in some cases it was larger than a simple sum of the 2. Furthermore, the current study places the results in the context of clinically relevant measures of ROM in a way in which the prior study was not designed to do. Whereas in all scenarios glenohumeral joint forces were larger and more posterior than when uninjured, impaired longitudinal growth more markedly influenced both postural and osseous deformity measures. Combined effects were larger than either in isolation. Treatments considering both mechanisms are warranted, although correction of growth restriction is more likely to influence ROM and osseous changes profoundly. This work not only provides insight into

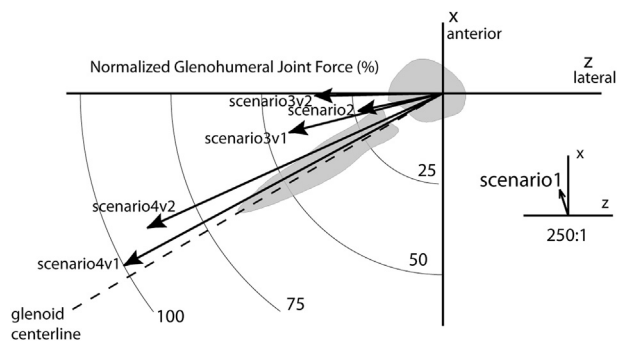


**FIGURE 2:** Joint forces in the transverse plane. Forces are shown normalized to the largest force in any simulation (scenario4v1) and relative to the scapula (gray silhouette). x is anterior and z is lateral. The vector of the uninjured scenario (scenario1) has been scaled by 250:1 for visualization because its magnitude is small relative to the other scenarios shown. In scenario2, when only muscle imbalance exists, the force is more compressive and posteriorly directed. Scenarios including restricted growth of affected muscles alone (scenario3) and in combination with muscle imbalance (scenario4) have forces of increasing magnitude and are increasingly posteriorly directed. When the entire subscapularis and teres major are considered to be affected (scenario3v1 and scenario4v1), the force is more posteriorly directed than when only the upper subscapularis is affected (scenario3v2 and scenario4v2).

the relative importance of 2 mechanisms acting at the shoulder; it also provides a biomechanical foundation to interpret and reconcile existing clinical literature that holds conflicting evidence regarding the causes of deformity.

Our results integrate with clinical observations of ROM in several ways. First, the magnitude of ROM restriction is similar to clinical observation. We predict external rotation reductions of 24° to 71°, similar to passive external rotation ROM restrictions seen clinically.<sup>4,32–35</sup> Reduced passive internal rotation has also been reported ( $17^\circ \pm 22^\circ$ ), as predicted in our simulations (0° to 16°). Passive internal rotation restriction was present only in scenarios involving impaired muscle growth. Therefore, impaired growth of denervated external rotators may explain posterior glenohumeral tightness that results in scapular winging during attempted internal rotation or cross-body adduction.<sup>36</sup> Second, our results reconcile conflicting MRI studies examining the relationship between muscle atrophy and shoulder contractures. One study found a correlation between shoulder internal rotation contracture severity and cross-sectional area ratio between internal rotators (pectoralis major and subscapularis) and external rotators (infraspinatus and teres minor).<sup>8</sup> Conversely, other MRI studies reported contracture severity to correlate

only with subscapularis atrophy rather than external rotators.<sup>6,7</sup> Despite conflicting conclusions, these studies share the MRI finding of atrophy of both external rotators and subscapularis that indicates neurologic injury to these muscles, which according to our model is sufficient to cause contractures through subsequent impaired growth, independent of muscle imbalance. Third, we did not find muscle imbalance alone to affect ROM substantially. This finding parallels clinical findings of a “notable absence” of contractures after C5–6 avulsion injuries.<sup>37</sup> In C5–6 nerve root avulsions, muscle imbalance identical to that after C5–6 nerve root ruptures fails to cause the contractures seen after C5–6 ruptures. This dichotomy could be explained by the preganglionic nature of these injuries, which preserves afferent muscle innervation, possibly preserving muscle growth.

Our simulations predicted glenohumeral joint forces consistent with increased glenoid retroversion and posterior humeral head subluxation.<sup>38</sup> In addition, relative severity of osseous deformity and ROM restriction were parallel among scenarios, similar to a clinically observed correlation between ROM and osseous deformity.<sup>33,39</sup> Whereas both muscle imbalance and impaired growth individually led to deforming forces, force magnitude increased synergistically when mechanisms were combined. However, the mechanisms may have different roles during stages of deformity development. It is possible that both mechanisms position the humeral head posteriorly whereas impaired muscle growth during skeletal growth drives the progressive nature of glenohumeral deformity with age.<sup>40</sup> Imbalance may gradually improve with neuromuscular recovery, whereas effects of muscle shortening would worsen with time and increased skeletal size.

Our simulations suggest that subscapularis impairment has an important role in overall outcome, because more negative outcomes were associated with a fully affected subscapularis. This is consistent with MRI evidence associating subscapularis atrophy with internal rotation contractures.<sup>6,7</sup> Evidence for subscapularis impairment includes atrophic appearance, increased fiber stiffness, and impaired growth in a mouse model of brachial plexus birth palsy.<sup>6,8,10,27</sup> Clinically, subscapularis release relieves shoulder internal rotation contractures after brachial plexus birth palsy.<sup>32,34,41</sup>

Our simulation had several limitations. First, our musculoskeletal model represented the anatomical geometry of an adult male. Therefore, we normalized joint forces for comparison between cases to eliminate the effect of different muscle forces between adults and

children. Second, our model assumed normal scapulothoracic kinematics and did not include changes to bony geometry or humeral head translation. Children with brachial plexus birth palsy have more scapulothoracic movement and smaller glenohumeral displacement to achieve internal/external rotation in clinical observation<sup>42</sup> and have glenoid retroversion. Our simulations were designed to limit the effect of these simplifications. For example, because shoulder posture was fixed and humeral head translation against the glenoid was not allowed, scapular kinematics and retroversion angle would have limited influence on outcome measures as we evaluated them. However, changes to glenoid version could change the effect of these directional forces on the bones, and humeral head translation may alter muscle actions and location of joint loading. Future work should examine humeral head translation in more detail. We did not take into account potential restrictive effects of pathological glenohumeral joint capsule or ligaments. However, numerous clinical reports describe successful release of internal rotation contracture by release of shoulder muscles alone,<sup>32,41,43</sup> especially the subscapularis, which highlights the primary role of musculature in contracture pathophysiology. We restricted our analyses to the transverse plane based on primary clinical reports of changes in glenoid retroversion and axial rotation ROM. However, abduction contractures also have been reported, sometimes severe enough to warrant varus osteotomy of the humerus.<sup>44</sup> Recent work reports that glenoid declination is prominent in these patients.<sup>35</sup> Therefore, future analyses of scapular plane changes are warranted. Finally, we applied uniform changes to muscles within affected and unaffected muscle groups, based on previous descriptions of the degree of imbalance<sup>8</sup> and shortening<sup>10</sup> exhibited after injury. We specifically chose values that reflected the best available estimate of these muscle changes; and in the case of imbalance, we used the largest reported value to highlight the most important effect that might be expected as a result of this mechanism. Individual muscles may be affected to different degrees given the pattern of injury for a particular patient. These simulations were intended to highlight the relative importance of possible underlying mechanisms of deformity, rather than to represent a specific patient.

The current work elucidates contributions to shoulder deformity and reconciles conflicting evidence in existing clinical literature. These simulations provide a foundation for future investigations into shoulder deformity, including both computational and

experimental work. For example, finite element analyses of bone growth and development under abnormal loading conditions may clarify the mechanobiological etiology and progression of bone deformity. Similarly, our study may inform animal model experiments that isolate the deformity mechanisms studied here to potentially identify methods to prevent or reverse deformity. Specifically, animal models can be used to determine the biological mechanisms by which the neurological injury alters postnatal muscle growth, because the current work highlights the importance of muscle growth on shoulder function and development after brachial plexus birth palsy.

### ACKNOWLEDGMENT

This work, including support for student effort, was supported by a research grant from the Pediatric Orthopaedic Society of North America and the Orthopaedic Research and Education Foundation.

### REFERENCES

- Hale HB, Bae DS, Waters PM. Current concepts in the management of brachial plexus birth palsy. *J Hand Surg Am.* 2010;35(2):322–331.
- Dodds SD, Wolfe SW. Perinatal brachial plexus palsy. *Curr Opin Pediatr.* 2000;12(1):40–47.
- Pearl ML. Shoulder problems in children with brachial plexus birth palsy: evaluation and management. *J Am Acad Orthop Surg.* 2009;17(4):242–254.
- Hoeksma AF, Ter Steeg AM, Dijkstra P, Nelissen RG, Beelen A, de Jong BA. Shoulder contracture and osseous deformity in obstetrical brachial plexus injuries. *J Bone Joint Surg Am.* 2003;85(2):316–322.
- Pearl ML, Edgerton BW. Glenoid deformity secondary to brachial plexus birth palsy: evaluation and management. *J Bone Joint Surg Am.* 1998;80(5):659–667.
- Hogendoorn S, van Overvest KL, Watt I, Duijsens AH, Nelissen RG. Structural changes in muscle and glenohumeral joint deformity in neonatal brachial plexus palsy. *J Bone Joint Surg Am.* 2010;92(4):935–942.
- Poyhia TH, Nietosvaara YA, Remes VM, Kirjavainen MO, Peltonen JI, Lamminen AE. MRI of rotator cuff muscle atrophy in relation to glenohumeral joint incongruence in brachial plexus birth injury. *Pediatr Radiol.* 2005;35(4):402–409.
- Waters PM, Monica JT, Earp BE, Zurakowski D, Bae DS. Correlation of radiographic muscle cross-sectional area with glenohumeral deformity in children with brachial plexus birth palsy. *J Bone Joint Surg Am.* 2009;91(10):2367–2375.
- Weekley H, Nikolaou S, Hu L, Eismann E, Wylie C, Cornwall R. The effects of denervation, reinnervation, and muscle imbalance on functional muscle length and elbow flexion contracture following neonatal brachial plexus injury. *J Orthop Res.* 2012;30(8):1335–1342.
- Nikolaou S, Peterson E, Kim A, Wylie C, Cornwall R. Impaired growth of denervated muscle contributes to contracture formation following neonatal brachial plexus injury. *J Bone Joint Surg Am.* 2011;93(5):461–470.
- Crouch DL, Plate JF, Li Z, Saul KR. Computational sensitivity analysis to identify muscles that can mechanically contribute to shoulder deformity following brachial plexus birth palsy. *J Hand Surg Am.* 2014;39(2):303–311.
- Holzbaier KR, Murray WM, Delp SL. A model of the upper extremity for simulating musculoskeletal surgery and analyzing neuromuscular control. *Ann Biomed Eng.* 2005;33(6):829–840.

13. Saul KR, Hu X, Goehler CM, et al. Benchmarking of dynamic simulation predictions in two software platforms using an upper limb musculoskeletal model. *Comput Methods Biomech Biomed Eng*. 2015;18(13):1445–1458.
14. Delp SL, Anderson FC, Arnold AS, et al. OpenSim: open-source software to create and analyze dynamic simulations of movement. *IEEE Trans Biomed Eng*. 2007;54(11):1940–1950.
15. Kato K. Innervation of the scapular muscles and its morphological significance in man. *Anatomischer Anzeiger*. 1989;168(2):155–168.
16. Murray WM, Buchanan TS, Delp SL. The isometric functional capacity of muscles that cross the elbow. *J Biomech*. 2000;33(8):943–952.
17. Jacobson MD, Raab R, Fazeli BM, Abrams RA, Botte MJ, Lieber RL. Architectural design of the human intrinsic hand muscles. *J Hand Surg Am*. 1992;17(5):804–809.
18. Lieber RL, Fazeli BM, Botte MJ. Architecture of selected wrist flexor and extensor muscles. *J Hand Surg Am*. 1990;15(2):244–250.
19. Lieber RL, Jacobson MD, Fazeli BM, Abrams RA, Botte MJ. Architecture of selected muscles of the arm and forearm: anatomy and implications for tendon transfer. *J Hand Surg Am*. 1992;17(5):787–798.
20. Holzbaur KR, Delp SL, Gold GE, Murray WM. Moment-generating capacity of upper limb muscles in healthy adults. *J Biomech*. 2007;40(11):2442–2449.
21. Holzbaur KR, Murray WM, Gold GE, Delp SL. Upper limb muscle volumes in adult subjects. *J Biomech*. 2007;40(4):742–749.
22. Langenderfer J, Jerabek SA, Thangamani VB, Kuhn JE, Hughes RE. Musculoskeletal parameters of muscles crossing the shoulder and elbow and the effect of sarcomere length sample size on estimation of optimal muscle length. *Clin Biomech (Bristol, Avon)*. 2004;19(7):664–670.
23. Rankin JW, Kwarcia AM, Mark Richter W, Neptune RR. The influence of altering push force effectiveness on upper extremity demand during wheelchair propulsion. *J Biomech*. 2010;43(14):2771–2779.
24. Poyhia TH, Koivikko MP, Peltonen JI, Kirjavainen MO, Lamminen AE, Nietosvaara AY. Muscle changes in brachial plexus birth injury with elbow flexion contracture: an MRI study. *Pediatr Radiol*. 2007;37(2):173–179.
25. Kim HM, Galatz LM, Das R, Patel N, Thomopoulos S. Musculoskeletal deformities secondary to neurotomy of the superior trunk of the brachial plexus in neonatal mice. *J Orthop Res*. 2010;28(10):1391–1398.
26. Soldado F, Fontecha CG, Marotta M, et al. The role of muscle imbalance in the pathogenesis of shoulder contracture after neonatal brachial plexus palsy: a study in a rat model. *J Shoulder Elbow Surg*. 2014;23(7):1003–1009.
27. Einarsson F, Hultgren T, Ljung BO, Runesson E, Friden J. Subscapularis muscle mechanics in children with obstetric brachial plexus palsy. *J Hand Surg Eur Vol*. 2008;33(4):507–512.
28. Sheffler LC, Lattanza L, Sison-Williamson M, James MA. Biceps brachii long head overactivity associated with elbow flexion contracture in brachial plexus birth palsy. *J Bone Joint Surg Am*. 2012;94(4):289–297.
29. Ballinger SG, Hoffer MM. Elbow flexion contracture in Erb's palsy. *J Child Neurol*. 1994;9(2):209–210.
30. Woo JS, Shin C, Hur MS, Kang BS, Park SY, Lee KS. Spinal origins of the nerve branches innervating the coracobrachialis muscle: clinical implications. *Surg Radiol Anat*. 2010;32(7):659–662.
31. Osbahr DC, Cannon DL, Speer KP. Retroversion of the humerus in the throwing shoulder of college baseball pitchers. *Am J Sports Med*. 2002;30(3):347–353.
32. Newman CJ, Morrison L, Lynch B, Hynes D. Outcome of subscapularis muscle release for shoulder contracture secondary to brachial plexus palsy at birth. *J Pediatr Orthop*. 2006;26(5):647–651.
33. Kozin SH. Correlation between external rotation of the glenohumeral joint and deformity after brachial plexus birth palsy. *J Pediatr Orthop*. 2004;24(2):189–193.
34. Pearl ML, Edgerton BW, Kazimiroff PA, Burchette RJ, Wong K. Arthroscopic release and latissimus dorsi transfer for shoulder internal rotation contractures and glenohumeral deformity secondary to brachial plexus birth palsy. *J Bone Joint Surg Am*. 2006;88(3):564–574.
35. Sheehan FT, Brochard S, Behnam AJ, Alter KE. Three-dimensional humeral morphologic alterations and atrophy associated with obstetrical brachial plexus palsy. *J Shoulder Elbow Surg*. 2014;23(5):708–719.
36. Russo SA, Loeffler BJ, Zlotolow DA, Kozin SH, Richards JG, Ashworth S. Limited glenohumeral cross-body adduction in children with brachial plexus birth palsy: a contributor to scapular winging. *J Pediatr Orthop*. 2014 Jul 2. [Epub ahead of print].
37. Al-Qattan MM. Obstetric brachial plexus palsy associated with breech delivery. *Annal Plast Surg*. 2003;51(3):257–264; discussion 265.
38. van Geleijn Vitranga VM, van Kooten EO, Mullender MG, van Doorn-Loogman MH, van der Sluijs JA. An MRI study on the relations between muscle atrophy, shoulder function and glenohumeral deformity in shoulders of children with obstetric brachial plexus injury. *J Brachial Plex Peripher Nerve Inj*. 2009;4:5.
39. Bhardwaj P, Burgess T, Sabapathy SR, Venkataramani H, Ilayaraja V. Correlation between clinical findings and CT scan parameters for shoulder deformities in birth brachial plexus palsy. *J Hand Surg Am*. 2013;38(8):1557–1566.
40. Dahlin LB, Erichs K, Andersson C, et al. Incidence of early posterior shoulder dislocation in brachial plexus birth palsy. *J Brachial Plex Peripher Nerve Inj*. 2007;2:24.
41. Bertelli JA. Lengthening of subscapularis and transfer of the lower trapezius in the correction of recurrent internal rotation contracture following obstetric brachial plexus palsy. *J Bone Joint Surg Br*. 2009;91(7):943–948.
42. Russo SA, Kozin SH, Zlotolow DA, et al. Scapulothoracic and glenohumeral contributions to motion in children with brachial plexus birth palsy. *J Shoulder Elbow Surg*. 2014;23(3):327–338.
43. Mehlman CT, Koepplinger ME. Hyphenated history: the Sever-L'Episcopo procedure. *J Pediatr Orthop*. 2007;27(5):533–536.
44. Waters PM, Bae DS. The effect of derotational humeral osteotomy on global shoulder function in brachial plexus birth palsy. *J Bone Joint Surg Am*. 2006;88(5):1035–1042.